Received: 29 July 2025 | Revised: 2 October 2025 | Accepted: 24 October 2025

DOI: 10.1002/ecs2.70506

ARTICLE

Vegetation Ecology

ECOSPHERE
AN ESA OPEN ACCESS JOURNAL

Microtopography and land management drive the spatial and population structures of a Mediterranean keystone species

Salvador Arenas-Castro | **Diego Jordano-Barbudo**

Área de Ecología, Departamento de Botánica, Ecología y Fisiología Vegetal, Facultad de Ciencias, Universidad de Córdoba, Córdoba, Spain

Correspondence
Salvador Arenas-Castro
Email: b62arcas@uco.es

Funding information
Ministerio de Ciencia, Innovación y Universidades, Grant/Award Number: TED2021-131722B-I00; ACUAVIR and IPA S.L.; Medidas compensatorias del embalse de la Breña II, Grant/Award Number: 400144; MCIN/AEI/10.13039/501100011033; European Union "NextGenerationEU"/PRTR

Handling Editor: Andrew J. Hacket-Pain

Abstract

Environmental and human factors shape the distribution and habitat of Mediterranean woody plants, influencing their population structure and conservation. The Iberian wild pear (*Pyrus bourgaeana*), a keystone fleshy-fruited species supporting wildlife during resource-scarce periods, is one such example. However, its habitat association and spatial patterns in Mediterranean managed woodland areas remain poorly understood. This study investigates its associations with microtopography and habitat heterogeneity in two key managed areas—dehesa (DEH) and abandoned olive grove (AOG)—within its core range in southern Spain. All trees ≥5 cm in diameter were mapped in a 223.3-ha plot, classified by size and age, and analyzed using spatial analysis, generalized linear models, and the torus translation test. Results showed stronger tree clustering in the AOG, with overall aggregation at small to intermediate scales (10–30 m), especially in older and larger trees. Positive associations were found between tree age, size, and microtopographic features. This light-demanding species preferred higher elevations and sunnier slopes. Human activities have significantly altered the species' structure: forest conversion to olive groves eliminated the Iberian wild pears, but abandonment allowed some regeneration via animal-dispersed seeds. However, increased ungulate density from hunting and cattle grazing, particularly in DEH, now severely limits regeneration, causing local declines. These findings highlight how historical land use and current grazing pressures affect the species viability and underscore the importance of targeted conservation strategies to preserve its role in Mediterranean ecosystems.

KEYWORDS

age and size structure, dendrochronology, habitat association, Mediterranean forest management, population structure, *Pyrus bourgaeana*, spatial analysis

This is an open access article under the terms of the Creative Commons Attribution License, which permits use, distribution and reproduction in any medium, provided the original work is properly cited.

© 2026 The Author(s). *Ecosphere* published by Wiley Periodicals LLC on behalf of The Ecological Society of America.

INTRODUCTION

Since the middle of the last century, rural landscapes in southern Europe have undergone rapid changes in land use. Human-induced changes in land use, in combination with climate change, are important drivers of Mediterranean vegetation dynamics (Chauchard et al., 2007; Peñuelas et al., 2017). This is the case of grasslands, dehesas (DEH) (open woodlands of *Quercus* species), and shrublands in the Mediterranean region, where the progressive management of the Mediterranean forest has been particularly intense and severe. In addition, depopulation of villages, which began during that period, continues to affect marginal regions with low productivity, leading to the abandonment of traditional agricultural and livestock practices (Quintas-Soriano et al., 2022). This has favored the natural regeneration and recovery of scrub and forest at the expense of crops and pastures (Gómez-García et al., 2023; Maestre et al., 2009).

These changes could become the drivers for the appearance and establishment of medium to small-sized trees that produce fleshy fruits (Rivest et al., 2011 and references therein), traditionally neglected in forest conservation but considered as keystones for the balance of the ecological networks of the Mediterranean ecosystem (Lombardo et al., 2020). But despite this apparent recovery of the Mediterranean undergrowth, a severe population decline of these woody plant species in these biomes has still been associated with land-use changes and the intensification of agricultural practices (Arenas-Castro et al., 2016; Weiner et al., 2011). In this sense, the correct management of Mediterranean forests and scrublands requires a solid understanding of their structure and dynamics, as well as rates of tree growth and productivity (Collado et al., 2023; Forner et al., 2018; Galván et al., 2014). Despite the drawbacks and problems involved in assessing the recruitment of most Mediterranean woody species or reconstructing their recent history, it is necessary to carry out a structural analysis based on the size and age of trees to estimate the stability of their populations. If we use age estimates as the basis of the structural analysis, we can reconstruct the details of the history of trees and regeneration patterns in the present and in the past, historical disturbances, or changes in land use (Peñuelas & Sardans, 2021; Rozas, 2003). Moreover, we must consider not only their structure and dynamics, but also how they are distributed in space, since anthropogenic disturbances decisively determine the spatial structure (Olthoff et al., 2018; Rozas et al., 2009), and this, in turn, is conditioned by the regeneration niches of the species involved in relation to environmental heterogeneity and modulated by biotic interactions (competition, herbivory, seed dispersal, seed predation, etc.) (Gill & Beardall, 2001). Furthermore, the sequence of disturbances that have taken place in the past can be reconstructed from radial growth patterns of trees, allowing us to test whether there is any temporal relationship between the occurrence of disturbances and regeneration (Colangelo et al., 2021; Pressey et al., 2007).

Nevertheless, the Mediterranean region is considered one of the hotspots for biodiversity (Médail et al., 2019; Myers et al., 2000), and although its forested areas are relict (McIntyre & Hobbs, 1999; Robin et al., 2021), populations often harbor unique endemic plant species. For all explained above, knowledge of the structure of Mediterranean woody species populations and their growth rates, especially medium-small fleshy fruit trees, is limited, or virtually null, in the case of some species such as the Iberian wild pear (*Pyrus bourgaeana* Decne. 1871–1872), an Ibero-Atlantic-Maghrebian Mediterranean endemism. This species is a small deciduous tree up to 8–10 m, with a broad and irregular crown, usually prickly, and leaves with a sawing margin. The Iberian wild pear is exclusive to the center and SW of the Iberian Peninsula and NW of the Maghreb (northern Africa). It is described as a sunny-tolerant species and well adapted to drought and prefers slightly acidic soils or very washed and reaches its optimum distribution in the Sierra Morena mountains (Andalusia, southern Spain) (http://www.floraiberica.org/). This species is particularly important for several reasons: first, it is classified as a characteristic species of the Mediterranean forests in Andalusia (Cabezudo & Pérez Latorre, 2004; Valdés et al., 1987) and is considered a habitual and diagnostic species of the meadows (DEH; Díaz & Pulido, 2009); second, this species could be playing an important trophic role because it provides valuable food resources in the form of palatable leaves, very attractive to vertebrate and invertebrate herbivores, and, what is more interesting, produces fleshy fruits during the summer when other resources are scarce (Arenas-Castro et al., 2016; Fedriani et al., 2010; Fedriani & Delibes, 2009). However, it is a scarce and rare species (Aedo & Aldasoro, 1998; Muñoz Garmendia & Navarro Aranda, 1998) with limited knowledge about its spatial distribution and niche ecology, and the ecological structure of most of its populations could be strongly affected by human-based disturbances (Arenas-Castro et al., 2016; Fedriani et al., 2023).

To address these concerns, we characterized the population structure (age and diameter classes) and analyzed the spatial patterns of *P. bourgaeana* at different life stages (juveniles [young], premature [middle age], and mature [old]) in a seminatural Mediterranean forest area in Sierra Morena mountain (southern Spain), with a focus on intraspecific spatial associations among the life stages and microtopographic attributes affecting. Due to

the recruitment mechanisms that the species shows, which can be vegetative or by propagules, as well as the dispersal mechanisms of its fruits and seeds either by wild or domestic fauna, we expect aggregated patterns between young and (semi-)adult trees. In addition, we also hypothesized that tree stands exhibit different types of spatial patterns that would be related to different types of management carried out in the study area. Finally, we hypothesize that this species has significant and specific habitat associations in the seminatural Mediterranean ecosystem. Our rationale was that the Iberian wild pear is not a habitat generalist species, and therefore, more cases of significant habitat association with life stages should appear indicating a better habitat definition.

Thus, our specific objectives were to (1) derive the tree stand density and determine the age–size structures; (2) detect the dynamic aspects of spatial pattern at different life stages and at different spatial scales; (3) reveal the spatial associations within different life stages considered; (4) check whether the spatial pattern of life stages is controlled by topographic/landform attributes and habitat heterogeneity; and (5) discuss the possible mechanisms, abiotic and/or human-induced, that contribute to the spatial patterns and associations with implications in natural regeneration of this species. The study could contribute to a better understanding of the complex ecosystem processes for maintaining the long-term stability and natural regeneration of the Iberian wild pear populations at the core of its distribution.

METHODS

Study area

The study area is a 225-ha estate devoted to extensive livestock husbandry and the pursuit of big game hunting located in the Sierra Morena mountain range (37°53′53.53″ N; 4°58′49.61″ W) in the province of Cordoba (Andalusia, southern Spain). The elevation ranges from 252 to 478 m above sea level (asl) (mean altitude = 349 m asl) and the average slope is 21.1% (66.3% maximum), with most slopes facing south. The climate of the area is Mediterranean, with extreme values during the summer season (Mesothermal climate). The annual precipitation ranges between 500 and 800 mm and is mainly concentrated in the winter months, with average temperatures ranging between 8 and 10°C. In summer, the precipitation ranges between 0 and 10 mm, and the monthly average temperatures vary between 25 and 26°C, with peak temperatures of up to 45° in July and August, which have become increasingly frequent in recent years (AEMET Spanish Meteorology Agency; https://www.aemet.es/es/portada). The soil is shallow and poorly developed, low in nutrients and organic matter content, and markedly acid. These soil features have led to land uses being centered on extensive livestock farming, game hunting, and forestry, with agricultural use almost negligible. In the study area, two distinct sections can be clearly delineated based on their topographical features, management practices, and vegetation structure (Figure 1).

The main section, approximately 75% of the study area, is occupied by the DEH, an open Mediterranean evergreen woodland of scattered Holm oak trees (*Quercus ilex* L. subsp. *ballota* [Desf.] Samp.) within a high diversity grassland. In the Iberian Peninsula, the DEH has been traditionally managed for cattle raising (Iberian pig, beef, sheep, and goat). However, in the last few decades, periodical shrub tillage by disc harrowing has been used to control shrub recruitment and regrowth, and grazing and browsing by cattle and wild herbivores (mainly roe deer) have dramatically increased. The second section covers most of the remaining study area and is occupied by an abandoned olive grove (AOG) (*Olea europaea* L.) that has been abandoned for over 50 years. There are still some remnant patches of semi-pristine Mediterranean forest of Holm oak and Cork oak (*Q. suber*) with a dense understory of Mediterranean shrubs.

Data collection and processing

Population structure and dendrochronological data

During May 2017, we identified and digitized the physical and geographical limits of the study area and both DEH and AOG sections using GIS tools (ESRI, 2015) on aerial images of 0.5 × 0.5 m spatial resolution. The whole area was divided into 25 × 25 m subplots, which would allow complete field sampling. In each subplot, all living individuals of *P. bourgaeana* with diameter at breast height (dbh) ≥ 5 cm or with height greater than 2 m were numbered with aluminum tags, gathering their respective data of dbh, crown diameter, and location coordinates. Georeferencing was carried out using a Trimble GeoXT Handheld GPS. Saplings and young trees <5 cm dbh were notably scarce throughout the entire expanse of the area.

Additionally, to estimate the age and growth of trees, we extracted two cores per tree with dbh ≥ 5 cm using a Haglöf Sweden increment borer 5 mm in diameter and 60 cm in length. The first core was extracted from the tree trunk at roughly 50 cm above the ground, on the

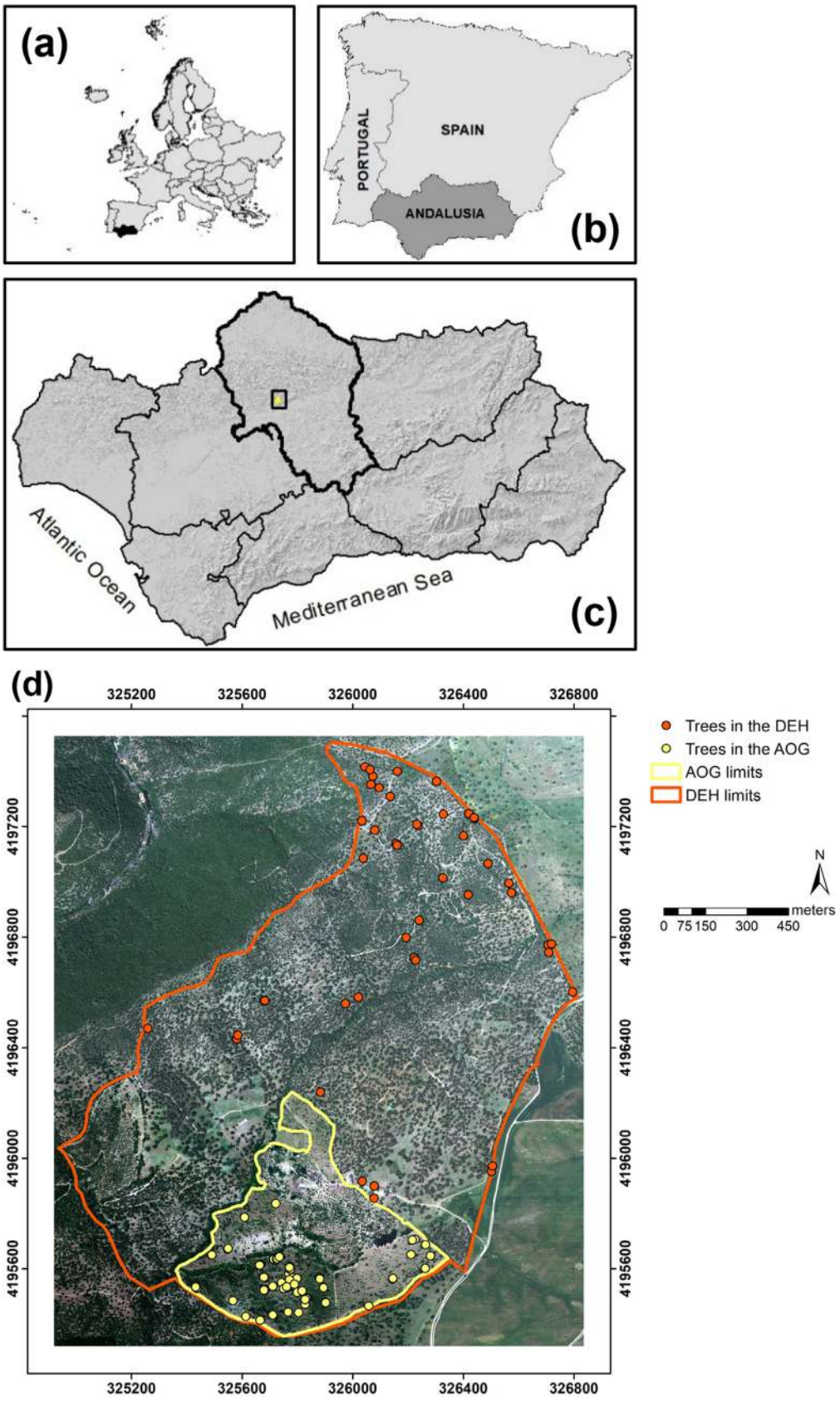


FIGURE 1 Location of the study area: (a) in the European context; (b) in Andalusia within the Iberian Peninsula context; (c) in the province of Cordoba (Andalusia); (d) georeferenced locations (spatial points) of individual trees within the two defined areas, the dehesa (DEH) and the abandoned olive grove (AOG). Photo credit: Salvador Arenas-Castro.

downslope-facing side, and the second one opposite the first and close to the ground. To obtain complete cores and minimize the chance of extracting cores with anomalous rings, the borer was inserted where the pith is farthest from the ground surface (Fritts, 1976). Core samples were properly labeled and mounted on wooden supports for sanding at the laboratory by standard techniques (Stokes, 1968) and subsequently scanned to obtain real size, high-resolution digital color images of each core. We applied the GIS-SDI method described in Arenas-Castro et al. (2015) to analyze these images with tools of free GIS software (DIVA-GIS), counting and measuring the growth rings—at least twice and independently for each core—allowing age and growth estimation (Swetnam et al., 1985). In addition, we applied a cross-dating quality control to tree ring series by using the COFECHA program (Grissino-Mayer, 2001) to ensure a correct estimation of the age and growth of the rings (Rozas, 2003). A total of 4467 tree rings on 244 cores (two per tree) were dated and measured.

Classification of age and diameter-size classes

In a previous study carried out in the same study area (Arenas-Castro et al., 2016), we demonstrated that the Iberian wild pear trees with a dbh ≥ 5 cm hosted, contrary to our expectations, a weak correlation between the age and dbh ($R^2 = 0.34$), proving dbh an unreliable predictor of age for this species. Thus, and for subsequent analyses, we used the estimated age and dbh values separately to classify the trees into life stages (based on age and size) as our response variable. Based on age, all individuals of *P. bourgaeana* with dbh ≥ 5 cm were classified into three age classes: Class I, young trees (≤20 years); Class II, middle-aged trees (21–40 years); Class III, old trees (>40 years). In terms of dbh, trees were categorized into three size classes: Class I, small trees (5–10 cm); Class II, medium trees (11–15 cm); Class III, large trees (>15 cm). Seedlings with a dbh < 5 cm, which were scarce throughout the area, were considered separately from the trees.

Calculation of topographic-geomorphometric predictors

To test how microtopographic attributes relate to life stages, we derived different topographic-geomorphometric predictors from the 5 × 5 m resolution PNOA digital elevation model (Plan Nacional de Ortofotografía Aérea, ftp://ftp.pnoa.ign.es/) for the study area: (1) seven topographic attributes (elevation, slope, aspect, eastness, northness, hillshade, flow direction of water) and (2) three landform heterogeneity variables (roughness, terrain ruggedness index, topographic position index) (Table 1). To obtain these variables, we used the function "terrain" available in the R package "raster" (version ≥3.5; Hijmans, 2025) and the R package "RSAGA" (version 1.3.0; Brenning et al., 2025). In the absence of micro-spatial data concerning other environmental variables in the study area (e.g., temperature or moisture), we derived these attributes as accurate predictors of the terrain profile. This characterization aids in understanding spatial and surface heterogeneity, as well as the abiotic environment, subsequently influencing hydrological, geomorphological, and biological processes (Hoersch et al., 2002; Stein & Kreft, 2015; Van Niel et al., 2004).

To avoid including highly correlated microtopographic variables in subsequent model fitting and retain independent predictors, we conducted a multicollinearity analysis by examining Spearman pair-wise correlations (<0.7) and variance inflation factors (VIF < 4) (Becker et al., 2015; Dormann et al., 2013) (Appendix S1: Figure S1). Given that generalized linear models (GLMs) can be sensitive to the number of predictors included in the modeling process (Sillero et al., 2021), and trying to maintain a tradeoff between the number of records and the number of variables per life stages (class of diameter and age), we selected four predictor variables for our models (Table 1).

Data analysis

Population structure and spatial point pattern analysis

To compare both ages and dbh classes between subplots (AOG vs. DEH), we used the Pearson's Chi-square test with statistical significance set at $p < 0.05$.

To analyze the spatial pattern of the Iberian wild pear trees, we firstly calculated the average nearest neighbor distance (NND) and the average nearest neighbor index (NNI) among trees using the "nndist" and "nni" functions from the "spatstat" (version 3.4-0; Baddeley et al., 2015) and "spatialEco" (version 2.0-2; Evans & Murphy, 2025) R-packages. This would show the point density and describe correlations among trees relative to their distances. The NND represents the average distance from each feature to its closest neighboring feature, while the NNI is the ratio of the observed distance to the expected distance. The expected distance is the average distance between neighbors in a hypothetical random distribution. A NNI < 1 indicates a clustering spatial pattern of trees; an index >1 suggests a trend toward dispersion or competition.

We also analyzed the level of aggregation and intraspecific spatial relations across different life stages (age

TABLE 1 Terrain-based topographic-geomorphometric attributes derived from a DEM at 5 × 5 m grid cell size to be related to different tree life stages by calculating generalized linear models (GLMs).

Name	Abbreviation	Description and role played on environmental and biodiversity modeling
Topographic		
Aspect	asp	Aspect usually refers to the direction of topographic slope faces. It is considered as an important contributor to vegetation and habitat types because affects the diversity and density of plant communities.
Northness[a]/ Eastness[a]	nness/eness	As aspect is a circular variable (0° and 360° represent the same thing—north), it is recommended to convert it into new variables: northness = cos(aspect) and eastness = sin (aspect). Northness will take values close to 1 if the aspect is mostly northward, close to −1 if the aspect is southward, and close to 0 if the aspect is either east or west. Eastness behaves similarly, except that values close to 1 represent east-facing slopes.
Elevation[a]	ele	Elevation is the distance above the sea level that may affect the type and amount of sunlight that plants receive, the amount of water that absorb and the nutrients that are available in the soil.
Flowdir	flowdir	This attribute returns the flow direction of water, that is, the direction of the greatest drop in elevation or the smallest rise if all neighbors are higher.
Hillshade	hshd	Hillshading uses light and dark areas to highlight where sunlight would hit and where shadows would form in the presence of hills and mountains. This attribute is an extremely useful technique to depict the topographic relief of a landscape, and robust indicator in describing and analyzing ecological processes by relying on soil moisture.
Slope	slo	Slope is the measure of steepness or the degree of inclination of a feature relative to the horizontal plane. It can affect vegetation growth by creating variation in solar-radiation incidence, wind velocity and soil type and by accelerating surface runoff and soil erosion.
Landform		
Topographic Position Index[a]	tpi	Topographic Position Index is the difference between a cell elevation value and the average elevation of the neighborhood around that cell. Positive values mean the cell is higher than its surroundings (ridgetops and hilltops), while negative values mean it is lower (valleys and canyon bottoms). Topographic Position Index values near zero could mean either a flat area or a mid-slope area.
Terrain Ruggedness Index	tri	Terrain Ruggedness Index represents the mean of the absolute differences between the value of a cell and the value of its surrounding cells. It informs about the terrain heterogeneity indicating how jagged or flat the terrain is on average. The Terrain Ruggedness Index is an important variable for predicting which habitats are used by species and the density at which species occurs across a variety of environments. Flat areas have a value of zero whereas mountain areas with steep ridges have positive values.
Roughness	rness	Roughness is defined as the difference between the maximum and the minimum value of a cell and its surrounding cells. It can modify the effect of the wind on the surface and physically protect part of the surface from abrasion caused by blowing particles. Presence or absence of soil surface roughness can also strongly influence water retention time at a given site, modifying the connectivity of water sources.

[a]Variable selected for model fitting.

and diameter) at multiple scales using spatial point pattern analysis with both single-variable and double-variable functions. For an overall approach, we employed Ripley's $L(r)$ function to examine the spatial distribution pattern of the Iberian wild pear in the study area. Ripley's $L(r)$ function, defined as $L(r) = (K(r)/\pi)^{1/2} - r$ (Besag, 1977), is an improvement over Ripley's $K(r)$ function (Upton & Fingleton, 1985; Wang et al., 2011). The $L(r)$ function transforms the theoretically expected value of a random distribution into a horizontal line that passes through point $P(0,0)$ and stabilizes the variance (Ripley, 1981), facilitating the interpretation of results via graphical representation of $L(r)$ versus r rather than the exponential $K(r)$ function. As both Ripley's $K(r)$ and $L(r)$ are cumulative functions, to adjust the null hypothesis to zero, it is necessary to transform $L(r)$ by subtracting the radius of the area of analysis, thats is, $L(r) - r$ (see Besag, 1977). In "spatstat" R package, it is necessary to transform K as $sqrt(./pi) - r \sim r$ to adjust the null hypothesis to zero. For a homogeneous Poisson process or Complete

Spatial Randomness (CSR), $K(r) = \pi r^2$ and $L(r) = 0$. $L(r) > 0$ indicates aggregation of the pattern at distance r, while $L(r) < 0$ suggests regularity of the pattern at distance r. Ripley's $L(r)$ function allows for simultaneous analysis of a species' spatial distribution pattern at any scale and is currently considered a pivotal method for population spatial distribution pattern analysis. This function evaluates the number of plant individuals within a circle centered on a point in the study area, with r representing the circle's radius. $L(r)$ values were calculated at 5-m intervals, approximating the maximum distance between neighbors. To correct the edge effects, we used the translation correction method implemented in the "spatstat" package, which is well suited for irregular plot boundaries and avoids the limitations of toroidal shift. Spatial randomness hypotheses were tested by simulating coordinates for several points with random distributions, matching the sample's individual count. We used the "envelope" function from the "spatstat" R package to simulate multiple realizations of the level of aggregation under the CSR hypothesis and compute the corresponding $L(r) - r$ values for each. The observed $L(r) - r$ from the actual data is then compared to the simulated envelope using a Monte Carlo test at the 0.05 level (a minimum of 99 simulations is required; Moeur, 1991), providing a visual and statistical tool to detect departures from CSR—such as clustering (when the observed curve lies above the envelope) or inhibition (when it lies below). Univariate analysis involving 999 simulations yielded a 99% CI for the spatial randomness hypothesis based on $L(r)$ maximum and minimum values at each distance r.

Given that spatial pattern analysis based on Ripley's K functions may not accurately represent information at small scales due to scale accumulation, we employed the *O-ring* function (Illian et al., 2008; Wiegand et al., 1999) for population structural pattern analysis. The *O-ring* function, a rescaled version of the pair correlation function $g(r)$ (Stoyan & Stoyan, 1994), utilizes rings instead of circles, effectively isolating specific distance classes and eliminating accumulation effects. The method provides an intuitive interpretation of the expected intensity of points at distance r from representative pattern points. We utilized the univariate *O-ring* function ($O_{11}(r)$) to analyze the spatial relationships within specific stage cohorts (young, middle-aged, and old), and the bivariate *O-ring* function ($O_{12}(r)$) to assess spatial relationships between different categories (Wiegand et al., 1999; Zhang et al., 2010). For the single-variable *O-ring* functions, the Heterogeneous Poisson Process (IPP) was used when trees exhibited clear aggregation; otherwise, Homogeneous Poisson Process (HPP) was used. For the double-variable *O-ring* functions, we selected an antecedent-condition null model, hypothesizing that older trees influence younger tree growth. The threshold spatial scale was set at 0–50 m based on preceding NND analysis. $O(r)$ values above the CI indicated clumped spatial distributions or positive correlations; values below suggested segregated or uniform spatial distributions or negative spatial correlation, and points within the CI implied random dispersions or independent correlations. Uni- and bivariate point patterns *O-ring* statistics were computed using the Programita 2018 software (Wiegand & Moloney, 2013).

Additionally, to assess the autocorrelation effect (Legendre & Legendre, 1998) and determine whether tree establishment in the study area occurred in age-based patches or continuously, we calculated Moran's I spatial autocorrelation coefficient across various distance classes (Duncan & Stewart, 1991; Frelich et al., 1993; Legendre & Fortin, 1989). We computed the standard normal deviations $Z(d)$ (Cliff & Ord, 1981) for this index. $Z(d)$ values greater than 1.96 indicate positive autocorrelation, while values less than −1.96 suggest negative autocorrelation. The overall significance test for each correlogram involved checking if at least one value was significant at the $0.05/k$ significance level, according to the Bonferroni criterion for multiple testing, where 0.05 is the correlogram overall significance level and k is the number of distance classes in the analysis. The spatial autocorrelation analysis based on Moran's I was conducted using the "sfdep" R package (version 0.2.4; Parry & Locke, 2024).

Relationships analyze between life stages and topographic factors and habitat association

We employed two different approaches (GLMs and torus translation test [TTT]) to evaluate the relationships between tree life stages, topographic/landform attributes, and habitat associations, respectively. Together, GLMs and TTT offer complementary insights: GLMs quantify relationships and predictor strength, while TTT validates whether observed associations exceed what would be expected by chance in a spatially structured environment. This combination strengthens ecological inference about how tree life stages respond to topography and relief and habitat conditions.

We used GLMs to relate the three different tree life stages (based on age and size) with microtopographic predictors. GLMs are versatile statistical tools for analyzing ecological relationships, as they account for the interactive behavior of variables that might not be adequately represented by classical Gaussian (linear) distributions (Guisan et al., 1999). Specifically, we fitted GLMs using the "glm" function of the "stats" R package (v3.6.2; R Core Team, 2013) with a gamma probability distribution given that the dependent variables (age and dbh) are skewed continuous data (>0) (Arenas-Castro et al., 2016).

To assess the performance of models, we used the "performance" R package (v0.6.1; Lüdecke et al., 2021), which provides utilities for computing measures (such as the corrected Akaike information criterion—AIC_c value) to assess and simultaneously compare model quality (e.g., r^2, intraclass correlation coefficient, root mean squared error and functions to diagnose overdispersion, among others). We also looked at the significance of each predictor for the response variables, aiming to identify the most influential contributors for each model.

To examine the habitat-species associations across life stages, we applied for the TTT. This test randomly calculates the distribution probability of a species within each habitat and tests whether the species is significantly related to the habitat by chance (see Harms et al., 2001; Zuleta et al., 2020 for details). In our study, we used the "classify_habitats" function from the "shar" R package (Hesselbarth, 2021) to delineate habitats based on a 25 × 25 m grid of quadrants within the study area, leveraging the elevation layer (digital elevation model [DEM]) with a spatial resolution of 5 × 5 m. This function takes the elevation raster as input and classifies it into discrete habitat classes based on defined breaks (in this case into five elevation classes). We selected 25 × 25 m blocks because our field sampling was carried out at this scale. We tested both positive and negative associations, defining significant positive associations when relative densities in the true habitat map exceeded 97.5% of the values from the TTT maps (α = 0.025 level of significance for a one-tailed test), and significant negative associations when the relative density in the true map fell below 2.5% of the TTT values. Subsequently, we accounted for positive and negative associations of each life stage with at least one habitat type.

RESULTS

Population structure and composition

The total number of living individuals recorded within the study area was 122 trees, with 72 in the AOG and 50 in the DEH. The tree density across the entire study area averaged one tree for every two hectares (Table 2). Notably, the AOG exhibited tree density nearly six times higher than that of DEH. Concerning the tree-age structure, the population displayed a pronounced bias and truncation in the younger age classes, with a complete absence of young trees (Class I: ≤20 years) in the AOG. In contrast, most of the trees in the DEH were in age class II (middle-aged trees; 21–40 years). On average, the trees exhibited a medium size with a mean dbh value of 17.4 ± 9.2 cm, ranging from 5.7 cm to 51.6 cm. However, the size frequency distributions differed between the AOG and DEH areas. The AOG predominantly featured trees in Class III (large trees; >15 cm), while the DEH was dominated by trees in Class I (small trees; 5–10 cm) (Figure 2). Pearson's χ^2 test reported significant differences in both age classes ($\chi^2 = 22.622$, df = 2, $p = 1.224e\text{-}05$) and dbh classes ($\chi^2 = 26.944$, df = 2, $p = 1.41e\text{-}06$) between the AOG and DEH.

Population distribution pattern

Points spatial pattern

The point density analysis revealed that over half of *Pyrus* trees in the olive grove were concentrated within a 50-m radius (Appendix S1: Figure S2). The average NND was three times shorter in the AOG compared to the DEH, indicating a more clustered distribution in the former subplot (Table 2). In contrast, the DEH exhibited a more scattered point pattern, with only two small groups of trees containing few individuals within a 50-m radius. In all cases, the NNI values were less than 1, suggesting a clustered distribution across the entire study area, as well as within the two subplots considered separately.

The univariate $L(r)$ function confirmed that the spatial distribution of trees was clearly aggregated across the overall study area (Figure 3a), as well as within the AOG and DEH (Figure 3b,c, respectively). Significant aggregations within the entire study area peaked between 10 and 30 m and transitioned to random distributions at intermediate and larger scales, with fluctuations occurring around 100 m. Specifically, trees in the AOG showed

TABLE 2 Summary of population structure and spatial pattern of all trees in both zones of the study area, dehesa (DEH) and abandoned olive grove (AOG).

Areas	*A*	N_t	*D*	NND	NNI	Age	dbh
AOG	43.1	72	1.7	17.79	0.50	49.8 ± 5.15	30.32 ± 6.85
DEH	180.2	50	0.3	50.36	0.46	41.6 ± 10.33	24.41 ± 8.44
Total	223.3	122	0.6	31.14	0.39	46.61 ± 11.91	28.15 ± 8.26

Note: Area (*A*; in hectares), tree number (N_t), density (*D*; N_t/area), nearest neighbor distance (NND; in meters), nearest neighbor index (NNI), age (mean ± SD in years) and diameter at breast height (dbh; mean ± SD in centimeters).

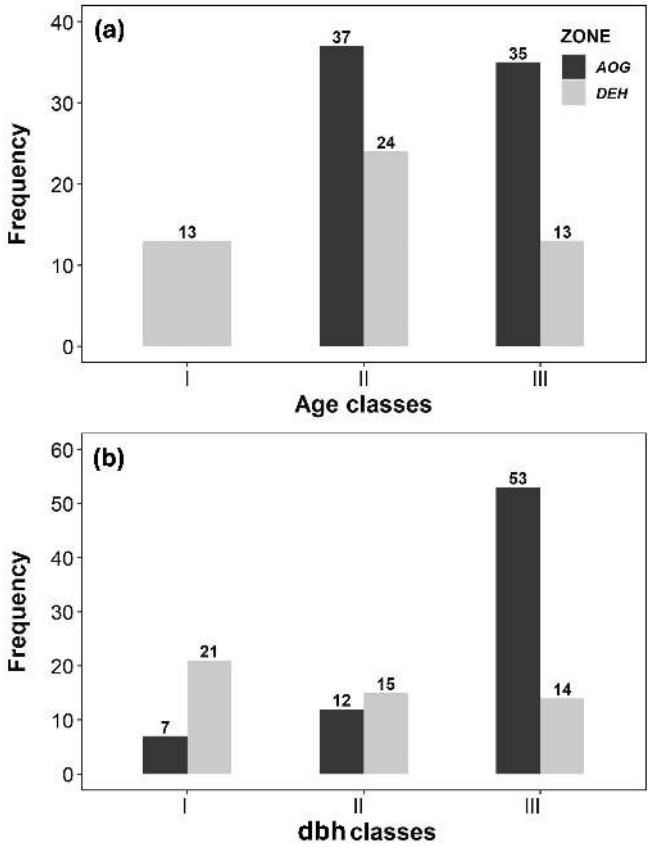


FIGURE 2 Frequency distribution of the Iberian wild pear trees per site (abandoned olive grove [AOG]; dehesa [DEH]) based on (a) age classes and (b) trees with dbh ≥ 5 cm. Age classes (years): I, ≤20; II, 21–40; III, >40. Diameter at breast height (dbh) classes (in centimeters): I, 5–10; II, 11–15; III, >15.

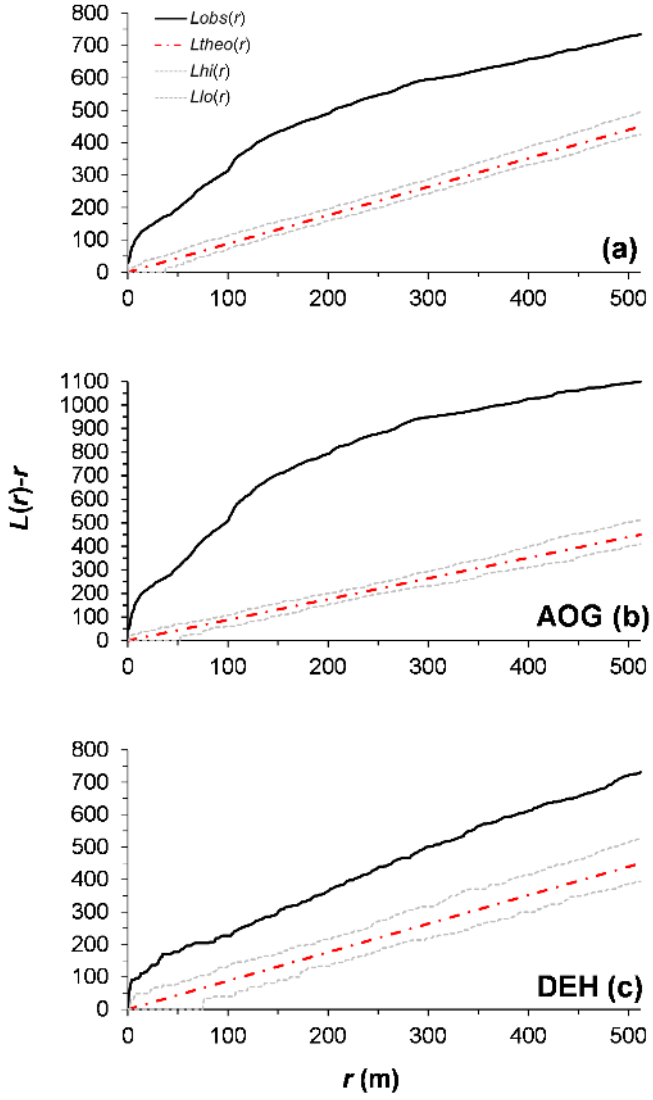


FIGURE 3 Spatial pattern of points for the (a) entire study area, (b) the abandoned olive grove (AOG), and (c) the dehesa (DEH) showing the empirical function $L(r)$ and the confidence limits at 95% for a random distribution (999 simulations). Positive values: spatial pattern in aggregates. Zero: random spatial pattern. Negative values: regular spatial pattern.

significant aggregations at 90 m, with the peak aggregation located around 20 and 30 m, while the DEH exhibited a maximum aggregation peak between 30 and 40 m and trended toward random distributions beyond 130 m.

The *O-ring* function analysis revealed that *P. bourgaeana* exhibited a strong aggregated distribution at small–middle scales, specifically less than 12–15 m, transitioning to a random distribution at greater distances (Figure 4a). Notably, trees within the AOG showed a slightly more clustered pattern compared to those in the DEH at shorter scales (Figure 4b,c, respectively).

Spatial structure of trees and associations based on age and size classes

We mapped the surveyed locations of *P. bourgaeana* across age and size classes (Figure 5a,b, respectively). These maps highlighted a heterogeneous and patchy distribution of both age and size classes throughout the study area. Although the DEH displayed slightly broader ranges, the relative homogeneity of age and size classes found in the AOG reaffirmed the aggregate pattern in both areas.

The single- and double-variable *O-ring* functions also allowed the analysis of spatial distribution and intraspecific spatial relationships among the age and size classes of *P. bourgaeana*. The univariate *O-ring* function revealed significant aggregations of trees at small scales, most notably in the AOG (Appendix S1: Figure S3), particularly around 5–10 m for middle-aged and older trees (II and III classes, respectively). A similar, albeit less pronounced pattern, was evident for trees in DEH across age classes I and II. Concerning diameter classes, only older

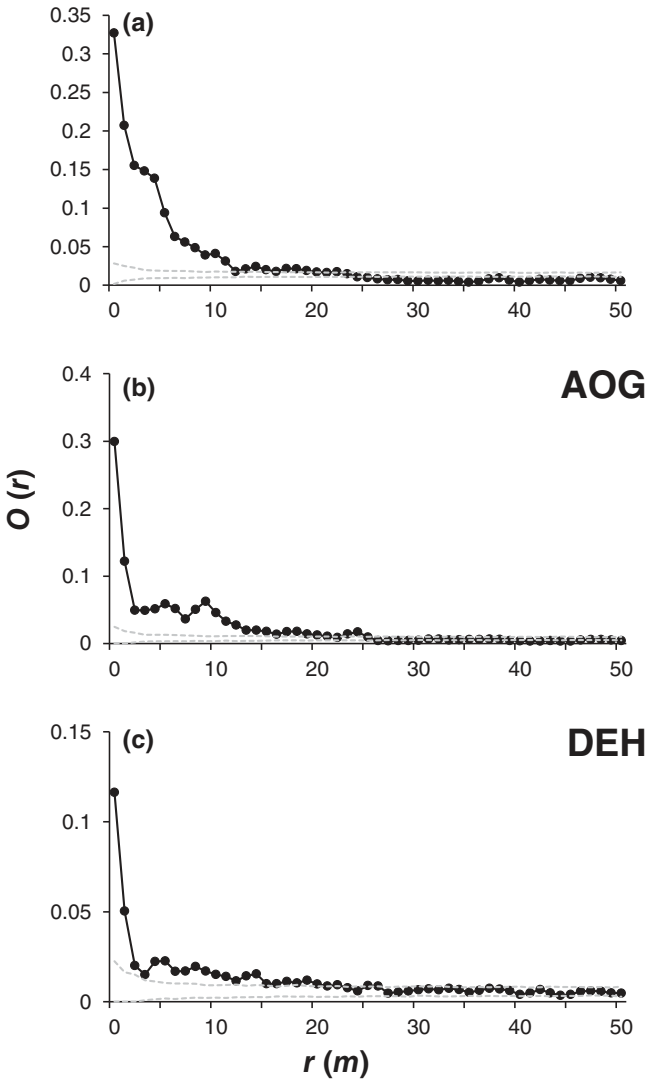


FIGURE 4 Pattern analysis by single-variable *O-ring* functions of *Pyrus bourgaeana* trees for the (a) entire study area, (b) the abandoned olive grove (AOG), and (c) the dehesa (DEH). Black lines with filled dots indicate univariate *O-ring* statistics ($O(r)$); gray dashed lines indicate upper and lower limits of the Monte Carlo simulations and repeated 999 times for a 95% CI in each process with the respective null model.

trees showed an aggregated pattern around 7–8 m in the AOG. In contrast, smaller and medium trees were clustered at shorter scales (2–3 m) and between 10 and 15 m in the DEH (Appendix S1: Figure S4).

Bivariate *O-ring* plots exploring spatial associations among tree life stages indicated that middle-aged trees in the AOG exhibited a spatially positive correlation with older adult trees at scales 7–8 m (Appendix S1: Figure S5). Conversely, no distinct association pattern was discernible among trees of varying age classes in the DEH. Regarding size classes, small trees in the AOG showed positive spatial associations with medium and large trees around 3–4 m (Appendix S1: Figure S6), whereas in DEH, significant correlations were only observed between small and medium-sized trees at larger scales (27–30 m).

In terms of spatial autocorrelation, the Moran's *I* correlogram for age in the AOG was not significant, suggesting an undefined spatial structure for the trees (Appendix S1: Figure S7). In contrast, the correlogram for *P. bourgaeana* age in the DEH was significant, indicating a positive autocorrelation across various spatial scales, particularly at distances up to 100 m, signifying the presence of tree groups with similar age structures.

Effects of topographic attributes on tree life stages

Overall, the tree life classes in the AOG were located at lower elevations compared to those in the DEH, ranging from 312.9 to 422.18 m asl, respectively (Appendix S1: Table S1). Although the trees grew on slopes with varying orientations, the tree density on north-facing slopes was around 1.43 times higher in the AOG than in the DEH. Interestingly, younger and smaller trees were predominantly found on south-facing slopes, whereas middle-aged and old-larger trees were less influenced by slope orientation (Appendix S1: Table S1).

The results of the GLM analysis elucidated the microtopographic effects on the life stages of the Iberian wild pear (Table 3). Overall, pseudo-R^2 indicated moderate-good fits (pseudo-$R^2 = 0.16$) for age and dbh, with values 0.2 and above typically considered good fits. Additionally, AIC values were lower than those of null models in some cases. Specifically, elevation exerted a consistent effect on half of age and dbh classes, with a significantly negative impact on age and a positive impact on dbh (Table 3) (Appendix S1: Figures S8 and S9). Regarding the aspect, only the eastness variable showed a significant effect on old trees (>40 years) as well as on small (5–10 cm) and large trees (>15 cm).

The TTT identified six habitat types based on elevation classes that we identified as the following types considering our knowledge of the study area: Hilltop, Ridges, Sunny and Shady slopes, Streamsides, and River basin. However, only five of these habitats were present within the study area (Figure 6). The most extensive habitat within the study area was Sunny slopes (84 ha; ~38% of the total study area), followed by Shady slopes (61 ha ~ 27.3%), Ridges (37 ha; ~16.6%), Hilltop (26 ha; ~11.6%) and Streamsides (15 ha; ~6.7%). Based on the TTT test results ($p < 0.01$), trees across all age and size classes displayed significant positive or negative associations with at least one habitat type (Table 4). Notably, only the younger and smaller size classes were positively associated with two habitats. The Shady slopes

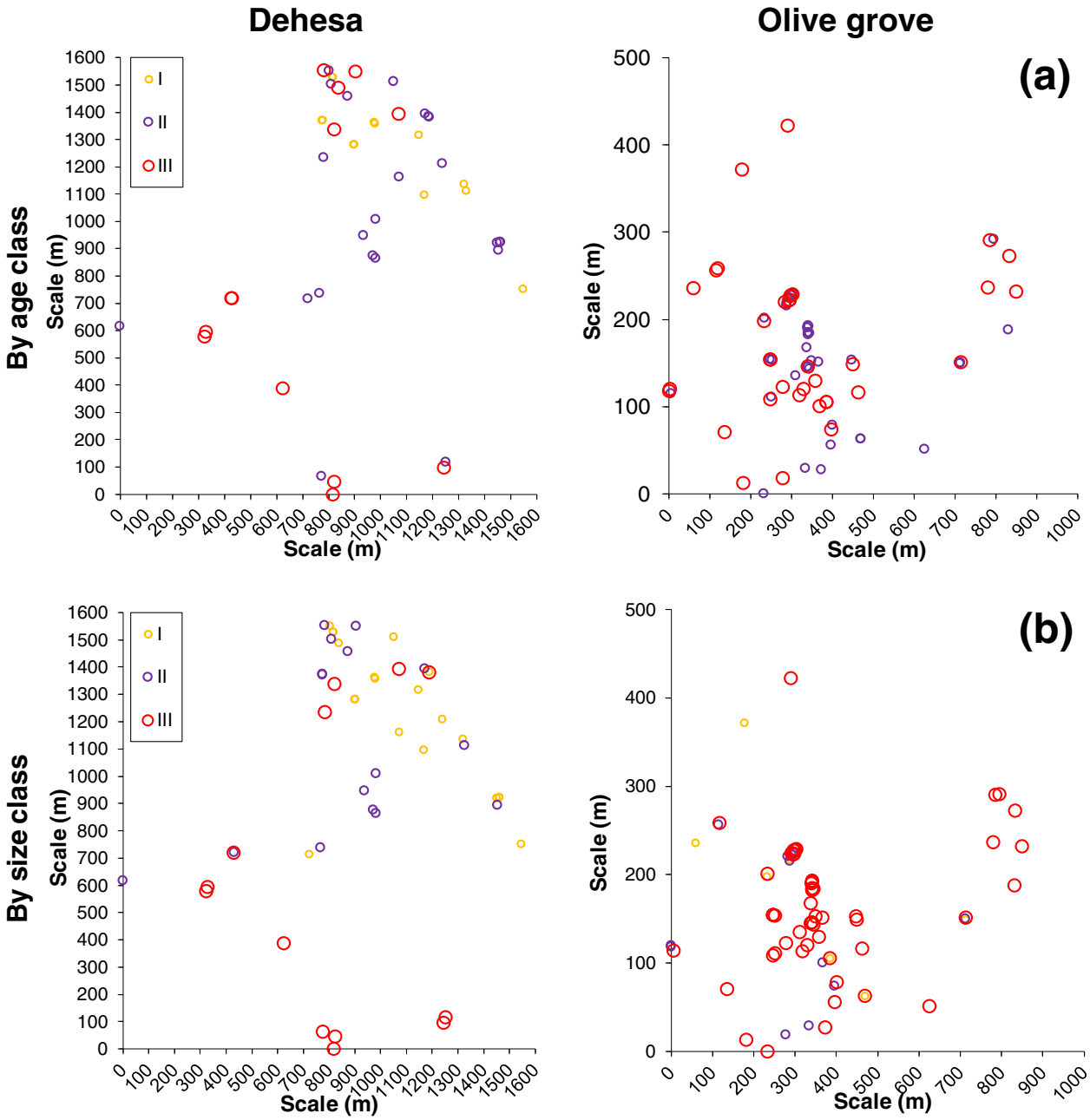


FIGURE 5 Spatial distribution points of trees in the study area (225 ha) based on (a) age (I, young trees, ≤20 years; II, middle-aged trees, 21–40 years; III, old trees, >40 years) and (b) dbh (I, small trees, 5–10 cm; II, medium trees, 11–15 cm; III, large trees, >15 cm).

habitat had the highest number of negative associations across all habitats (Table 4), mainly among the age-based life stages (Figure 6). Conversely, Hilltop and Sunny slopes habitats exhibited a higher frequency of positive associations compared to the other habitats.

DISCUSSION

This study aimed to quantitatively assess whether microtopographic attributes and habitat heterogeneity shape the regeneration of the Iberian wild pear at a fine scale within its distribution core, with the hypothesis that tree stands exhibit different types of spatial patterns that would be related to different types of human management carried out in the study area, DEH and AOG. Overall, our findings substantially supported our hypotheses as the absence of saplings and the prevalence of middle-aged and old trees indicate a clear collapse of recruitment in the last decades, attributable to the intensification of sheep browsing and an increase in deer density, strongly associated with human management

TABLE 3 Results from the generalized linear models (GLMs) explaining the microtopographic effects on life stages (age and dbh) of the Iberian wild pear.

Life stage	*N*	AIC_c	AIC_{N0}	Pseudo-R^2	Coefficients			
					ele	eness	nness	tpi
Age								
I	13	71.72	68.83	0.26	0.00	−1.65	0.48	13.38
II	61	380.21	379.41	0.11	**−0.03(.)**	−0.49	−0.21	−9.63
III	48	322.69	328.98	0.26	−0.00	**−0.00(***)**	0.00	−0.00
All	122	940.41	953.85	0.16	**−0.09(***)**	−0.27	−0.16	9.36
dbh								
I	28	109.41	108.69	0.21	0.00	**−0.93(.)**	0.38	1.59
II	27	109.64	104.48	0.10	−0.00	0.47	0.53	−1.56
III	67	474.03	473.94	0.09	0.00	**−0.01(.)**	0.00	0.01
All	122	877.06	889.97	0.16	**0.00(**)**	−0.00	−0.01	0.03

Note: Coefficients, estimate and *p*-value. See Table 1 for explanations of attribute abbreviations. The significant pair-wise differences are shown in boldface.
***$p < 0.001$; **$p < 0.01$; "." $p < 0.1$.
Abbreviations: AIC_c, corrected Akaike information criterion value; AIC_{N0}, a baseline "null model" containing a single intercept term; *N*, number of individuals; Pseudo-R^2, the proportion of the explained deviance by the model.

practices. However, both topographic and habitat heterogeneity differently drove the spatial and ecological distribution of species' life stages in both DEH and AOG subplots. These results highlight the importance of intensive land management in shaping the Iberian wild pear spatial pattern even inside a protected area, while also suggesting that other environmental factors at microscale may modulate their level of aggregation and habitat associations.

Tree life stages and spatial patterns

Although the AOG subplot constitutes only 19.3% of the study area, tree density was nearly three times higher than in the DEH subplot, hosting 59% of all old trees. No evidence of small trees was found in the AOG, and both the II (21–40 years) and III (>40 years) age classes showed similar frequencies. *P. bourgaeana* trees predominated in the middle age classes within the DEH, suggesting a relatively stable population, albeit with a size distribution skewed toward smaller tree classes. Furthermore, trees in the AOG were smaller than those in the DEH for small (5–10 cm) and medium (11–15 cm) size classes, but significantly larger for large trees (>15 cm), approximating a J-shaped distribution.

The low frequency of trees in the younger age classes evidences the null or very low recruitment in recent years, leading to a clearly biased demographic structure, resulting in an inverted or regressive age pyramid inherent to aging populations. This pattern was evident in both the AOG and DEH tree groups and can be explained by the historical forest management practices prevalent in most mountainous areas in Sierra Morena (Arenas-Castro et al., 2016). Traditional land uses focused on extensive livestock farming in the DEH and olive cultivation, occasionally supplemented by big game hunting and cork extraction (Martínez-Sastre et al., 2017). However, most of these activities were abandoned 20–25 years before our field work, as observed in the AOG, in favor of intensive livestock farming characterized by continuous and severe grazing pressure on natural vegetation. The age frequency distribution of the Iberian wild pear trees, with well-represented age classes between 35 and 50 years, suggests that changes in land management practices provided a temporal window for slight regeneration of the Iberian wild pear trees. Dendrochronological analysis indicates that 51.4% of the trees were established over a 10-year period between 1973 and 1983 (Arenas-Castro et al., 2015, 2016). Consequently, the current AOG population results from natural regeneration following the abandonment of tillage and olive grove management. Conversely, the age distribution of the Iberian wild pears in the DEH differs from that in the AOG, indicating slightly higher stability and moderate recruitment over the past 20–30 years. Thus, different land use changes in these two subplots have shaped the current population structure of this species. Furthermore, this suggests a significant potential for the Iberian wild pear to colonize disturbed areas (Arenas-Castro et al., 2016), despite limitations imposed by fenced hunting areas with excessive ungulate grazing

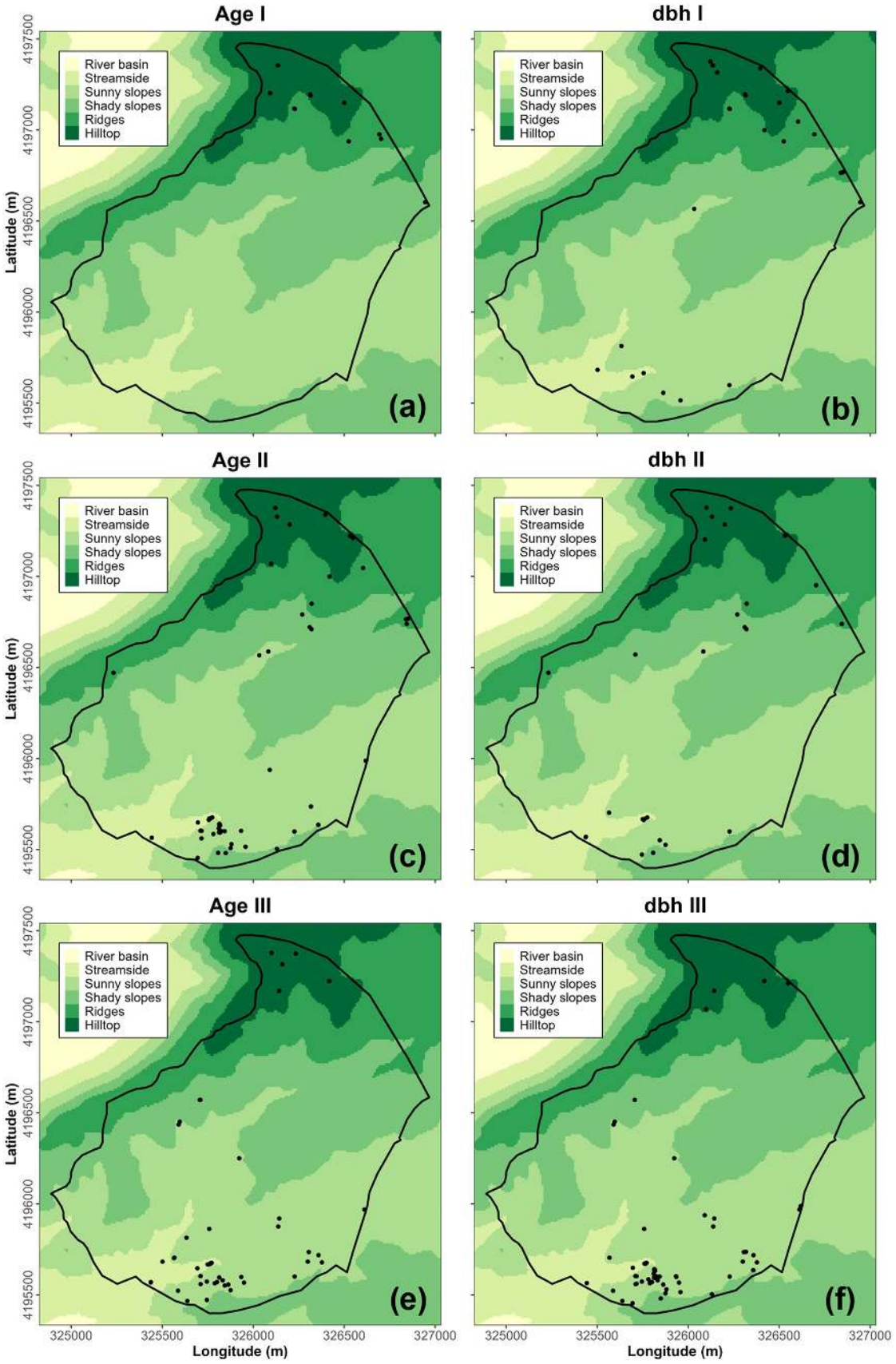


FIGURE 6 Maps of the six habitat types calculated in the study area based on 25 × 25 m blocks. Black dots represent each tree per life stage. Age: (a) I, young trees, ≤20 years; (c) II, middle-aged trees, 21–40 years; and (e) III, old trees, >40 years. Diameter at breast height (dbh): (b) I, small trees, 5–10 cm; (d) II, medium trees, 11–15 cm; and (f) III, large trees, >15 cm.

TABLE 4 Species-habitat associations of three different life stages per age (I, young trees, ≤20 years; II, middle-aged trees, 21–40 years; III, old trees, >40 years) and dbh (I, small trees, 5–10 cm; II, medium trees, 11–15 cm; III, large trees, >15 cm) in each habitat type.

	Habitat type				
Life stage	**Hilltop**	**Ridges**	**Shady slopes**	**Sunny slopes**	**Streamsides**
Age					
I	+	*N*	−	+	*N*
II	−	*N*	−	*N*	*N*
III	*N*	*N*	−	+	*N*
dbh					
I	+	*N*	*N*	+	*N*
II	*N*	*N*	−	*N*	*N*
III	*N*	*N*	*N*	+	*N*

Note: +, −, and *N* indicate positive associations (>99.5%), negative associations (<0.005%), and no corresponding associations, respectively.

pressure and land fragmentation on seed dispersal and regeneration of these fleshy fruit species (Morera et al., 2025; Muñoz et al., 2017).

Intraspecific spatial patterns and associations among life stages

Overall, trees exhibited a clearly clustered pattern across the whole study area, as evidenced by NND analysis, as well as by the $L(r)$ function and the (uni-)bivariate correlation *O-ring* function analysis. Maximum levels of significant aggregation were detected around 20–40 m. Clustering was more pronounced in the AOG, with a strong clustered pattern at shorter scales (around 12–15 m) and over half of the trees concentrated within a 50-m radius. In contrast, trees in the DEH were more dispersed, with only two small groups detected within a 50-m radius.

Our findings confirm that Iberian wild pear trees were scattered, with distances of up to 80–100 m between nearest neighbors, yet also form patches comprising closely spaced individuals. Age-based spatial patterns showed significant aggregations at small scales (~5–10 m) for the middle-aged (21–40 years) and older trees (>40 years) in the AOG, while similar clustering was observed in the DEH for young (≤20 years) and middle-aged classes. Regarding size classes, small trees exhibited positive spatial associations with medium and large trees (around 3–4 m) in the AOG, whereas this association was only evident at larger scales (~ 30 m) for small and medium-sized trees in the DEH.

Interestingly, intraspecific competition, often a key factor shaping spatial structure in tree populations, did not appear significant in our Iberian wild pear population, as evidenced by the absence of significant positive autocorrelation among tree ages at short distances. This spatial structure contrasts with that observed in dense temperate forests where intense intraspecific competition leads to strong positive autocorrelation over short distances and negative autocorrelation at intermediate and large distances (Fox et al., 2007; Pommerening et al., 2021). In the AOG, old trees can grow in dense aggregates without apparent intraspecific competition issues. The formation of these patches may be influenced by endozoochorous seed dispersion resulting in contagious distributions (Fedriani & Delibes, 2009), or because the distribution of suitable sites for the establishment of seedlings was patched. Additionally, in both subplots, we found two different dense patches of apparent saplings, but removing the soil around them we verified that they were suckers still connected by their roots, growing next to injured or cut adult trees (author's observations). Therefore, root disturbance by disc harrowing or damage to individual trees may promote vegetative propagation by regrowth from the roots, leading to the formation of dense stands of trees. Asexual reproduction has been well documented in Mediterranean species within the *Rosaceae* (Rasmussen & Kollmann, 2007; Vik et al., 2010). The ability to regrow from the roots provides resilience against disturbances (Kolb & Diekmann, 2005; Peterson & Pickett, 2000), but it is not considered a viable alternative to recruitment (Espelta et al., 2003).

Microtopographic attributes influence the life stages and species-habitat associations

Our analysis also identified specific relationships between tree life stages and topographic attributes and habitat types. Although trees were found across all exposures, 48.4% of them were located on north-facing slopes

(consistent with the predominant orientation of the AOG), compared to only 27% on south-facing slopes, despite their greater extent (108 vs. 30 ha). However, GLM results indicated a significant preference for sun-exposed orientations among different life stages. Specifically, young (≤20 years) and smaller trees (5–10 cm dbh) were more prevalent on south-facing slopes than middle-aged (21–40 years) and larger trees (>40 years). Models also showed a significant relationship between elevation and trees, but the sign varied depending on age and dbh life stage classes: negative and positive, respectively. The GLM results were confirmed by the TTT approach. According to the TTT, more than half of the life stages were significantly positively or negatively correlated with two habitat types. The TTT also confirmed that the Iberian wild pear avoids shady areas in favor of sun-exposed sides, corroborating the thermophilic nature of this species. Specifically, both the young and the smaller trees, as well as older and larger trees, were positively associated with the Sunny slopes habitat type. In contrast, trees did not show any association with ridges or stream areas but displayed a strong negative association with shaded areas.

Most species exhibit distinct habitat associations across different life stages, suggesting that these associations play a role in shaping the regeneration niche and influencing species coexistence (De Reu et al., 2013; Hesselbarth & Wiegand, 2024). We therefore highlight the importance of micro environmental features, such as elevation and topography, as crucial drivers of habitat heterogeneity for this light-demanding Iberian wild pear species (Aryal et al., 2017; Nadal-Romero et al., 2014). In this population, elevation likely influences soil water and nutrient content from the valley to the ridgetop, while topography also serves as a first-order control on spatial variation in hydrological conditions that affect the spatial pattern of nutrients and soil moisture, thus influencing tree life stages. In other words, although this species is usually adapted to stressful environments with exposed conditions of high light and temperature, and thin soils often exposed rock with siliceous concentrations, it also appears in fresh areas where a certain amount of moisture is retained. Our results demonstrate that the habitat association of the Iberian wild pear in the study area overall changed with different life stages.

CONCLUSION

In summary, the life stage structure of the Iberian wild pear population has been and continues to be strongly influenced by land management and changing land uses carried out in the study area for over 50 years. Agricultural use initially involved the clearing of natural vegetation, tillage, and planting olive trees; later, periodical tilling and additional uses followed. This type of management hinders the natural regeneration of Mediterranean woody species, including the Iberian wild pear. After the tilling was abandoned, significant recruitment occurred, resulting in the primary core of trees that exists today. This recruitment began to decrease with the onset of livestock use and was severely restricted with its intensification, jeopardizing the persistence of these populations. While it is challenging to generalize our results to the entire distribution area of this species, we anticipate significant variability in the age structure of different populations of the Iberian wild pear across its geographical range. The species' distribution core lies in southwestern Sierra Morena (Andalusia), which encompasses a diverse mosaic of ecological units subject to different uses and management practices (hunting, livestock, forestry, agriculture, and others). On many farmlands, regardless of hunting use, intensive livestock grazing persists, and it is foreseeable that under these conditions the age structure of the Iberian wild pear is truncated, with minimal or no representation of trees in the younger age classes. We further predict that in areas where livestock farming, especially goats and sheep, has been the primary traditional use, and in fenced hunting areas of Sierra Morena with high densities of deer and wild boars, the presence of the Iberian wild pear will likely be minimal. However, until now, knowledge about the biology and ecology of *P. bourgaeana* has been virtually nonexistent. Our results offer new insights into the demography of this fleshy fruit tree, a rare and poorly known species in core populations from West Sierra Morena. These findings are relevant for understanding the effects of agricultural and livestock practices on the species' population dynamics and spatial distribution, which could compromise the long-term viability of the species' populations, providing important implications from its conservation standpoint.

AUTHOR CONTRIBUTIONS

Salvador Arenas-Castro: conceptualization (equal); data curation (lead); formal analysis (lead); investigation (lead); methodology (lead); visualization (lead); validation (lead); software (lead); writing—original draft (lead); writing—review and editing (lead). **Diego Jordano-Barbudo:** funding acquisition (lead); investigation (supporting); project administration (lead); supervision (lead); writing—original draft (supporting); writing—review and editing (supporting). Both authors gave their final approval for publication.

ACKNOWLEDGMENTS

We thank the conservation director of the Hornachuelos Natural Park (Córdoba, Spain) for providing logistical support during the fieldwork.

FUNDING INFORMATION

This research was funded by the ACUAVIR and IPA S.L. companies and Junta de Andalucia (Spain) as part of the project "Medidas compensatorias del embalse de la Breña II" (grant number 400144). This publication is also part of the FORMEDY project (TED2021-131722B-I00), funded by MCIN/AEI/10.13039/501100011033 and by the European Union "NextGenerationEU"/PRTR. Recovery, Transformation and Resilience Plan – Funded by the European Union—NextGenerationEU. Salvador Arenas-Castro was supported by the María Zambrano program funded by the Spanish Ministry of Universities and the University of Córdoba (Spain) (Next Generation EU fund).

CONFLICT OF INTEREST STATEMENT

The authors declare no conflicts of interest.

DATA AVAILABILITY STATEMENT

A sample of data and code (Arenas-Castro, 2025) is available from Zenodo: https://doi.org/10.5281/zenodo.16325051. The full species datasets generated and analyzed during the current study are not publicly available due to the sensitivity of the study area (the Hornachuelos Natural Park; Córdoba, Spain). Qualified researchers may contact the Department of Botany, Ecology and Plant Physiology (University of Cordoba, Spain; https://www.uco.es/botanica/es/) to request access. All environmental data are openly available on each corresponding website.

ORCID

Salvador Arenas-Castro https://orcid.org/0000-0001-8671-4968

REFERENCES

Aedo, C., and J. J. Aldasoro. 1998. *Flora Ibérica: Plantas Vasculares de La Península Ibérica e Islas Baleares, Vol. 6. Rosaceae*. Madrid: Real Jardín Botánico-CSIC.

Arenas-Castro, S. 2025. "Salvador-Arenas-Castro/Micro-Scale-Habitat-Association: Data and Code for 'Microtopography and Land Management Drive the Spatial and population Structures of a Mediterranean Keystone Species'." Data Set. Zenodo. https://doi.org/10.5281/zenodo.16325051

Arenas-Castro, S., J. Fernández-Haeger, and D. Jordano-Barbudo. 2015. "A Method for Tree-Ring Analysis Using Diva-Gis Freeware on Scanned Core Images." *Tree-Ring Research* 71(2): 118–129.

Arenas-Castro, S., J. Fernández-Haeger, and D. Jordano-Barbudo. 2016. "Population Structure and Fruit Production of *Pyrus bourgaeana* D. Are Affected by Land-Use." *Acta Oecologica* 77: 91–99.

Aryal, R. R., H. Latifi, M. Heurich, and M. Hahn. 2017. "Impact of Slope, Aspect, and Habitat-Type on LiDAR-Derived Digital Terrain Models in a Near Natural, Heterogeneous Temperate Forest." *PFG – Journal of Photogrammetry, Remote Sensing and Geoinformation Science* 85(4): 243–255.

Baddeley, A., E. Rubak, and R. Turner. 2015. *Spatial Point Patterns: Methodology and Applications with R*. London: Chapman and Hall/CRC Press.

Becker, J.-M., C. M. Ringle, M. Sarstedt, and F. Völckner. 2015. "How Collinearity Affects Mixture Regression Results." *Marketing Letters* 26(4): 643–659.

Besag, J. 1977. "Contribution to the Discussion on Dr. Ripley's Paper." *Journals of the Royal Statistical Society B* 39: 193–95.

Brenning, A., D. Bangs, and M. Becker. 2025. "RSAGA: SAGA Geoprocessing and Terrain Analysis." R Package Version 1.4.2, https://github.com/r-spatial/rsaga.

Cabezudo, B., and B. Pérez Latorre. 2004. "Las Comunidades Vegetales." In *El Monte Mediterráneo En Andalucía* 29–39. Sevilla: Consejería de Medio Ambiente, Junta de Andalucía.

Chauchard, S., C. Carcaillet, and F. Guibal. 2007. "Patterns of Land-Use Abandonment Control Tree-Recruitment and Forest Dynamics in Mediterranean Mountains." *Ecosystems* 10(6): 936–948.

Cliff, A. D., and J. K. Ord. 1981. *Spatial Processes: Models & Applications* 266. London: Pion Ltd.

Colangelo, M., J. J. Camarero, A. Gazol, G. Piovesan, M. Borghetti, M. Baliva, T. Gentilesca, A. Rita, A. Schettino, and F. Ripullone. 2021. "Mediterranean Old-Growth Forests Exhibit Resistance to Climate Warming." *Science of the Total Environment* 801: 149684.

Collado, E., M. Piqué, J. Coello, J. de-Dios-García, C. Fuentes, and L. Coll. 2023. "Close-to-Nature Management Effects on Tree Growth and Soil Moisture in Mediterranean Mixed Forests." *Forest Ecology and Management* 549: 121457.

De Reu, J., J. Bourgeois, M. Bats, A. Zwertvaegher, V. Gelorini, P. De Smedt, W. Chu, et al. 2013. "Application of the Topographic Position Index to Heterogeneous Landscapes." *Geomorphology* 186: 39–49.

Díaz, M., and F. J. Pulido. 2009. "Dehesas Perennifolias de *Quercus* spp." In *Bases Ecologicas Preliminares Para La Conservación de Los Tipos de Hábitat de Interés Comunitario En España*, Vol. 69. Madrid: Ministerio de Medio Ambiente y Medio Rural y Marino.

Dormann, C. F., J. Elith, S. Bacher, C. Buchmann, G. Carl, G. Carré, J. R. García Marquéz, et al. 2013. "Collinearity: A Review of Methods to Deal with It and a Simulation Study Evaluating Their Performance." *Ecography* 36(1): 27–46.

Duncan, R. P., and G. H. Stewart. 1991. "The Temporal and Spatial Analysis of Tree Age Distributions." *Canadian Journal of Forest Research* 21: 1703–10.

Espelta, J. M., J. Retana, and A. Habrouk. 2003. "Resprouting Patterns after Fire and Response to Stool Cleaning of Two Coexisting Mediterranean Oaks with Contrasting Leaf Habits on Two Different Sites." *Forest Ecology and Management* 179(1): 401–414.

Evans, J. S., and M. A. Murphy. 2025. "spatialEco." R Package Version 2.0–3. https://github.com/jeffreyevans/spatialEco

Fedriani, J. M., and M. Delibes. 2009. "Seed Dispersal in the Iberian Pear, *Pyrus bourgaeana*: A Role for Infrequent Mutualists." *Écoscience* 16(3): 311–321.

Fedriani, J. M., T. Wiegand, and M. Delibes. 2010. "Spatial Pattern of Adult Trees and the Mammal-Generated Seed Rain in the Iberian Pear." *Ecography* 33(3): 545–555.

Fedriani, J. M., T. Wiegand, P. J. Garrote, M. J. Leiva, and D. Ayllón. 2023. "Seed Dispersal Effectiveness in Fragmented and Defaunated Landscapes." *Ecosphere* 14(9): e4658.

Forner, A., F. Valladares, D. Bonal, A. Granier, C. Grossiord, and I. Aranda. 2018. "Extreme Droughts Affecting Mediterranean Tree Species' Growth and Water-Use Efficiency: The Importance of Timing." *Tree Physiology* 38(8): 1127–37.

Fox, J. C., H. Bi, and P. K. Ades. 2007. "Spatial Dependence and Individual-Tree Growth Models: I. Characterising Spatial Dependence." *Forest Ecology and Management* 245(1): 10–19.

Frelich, L. E., R. R. Calcote, M. B. Davis, and J. Pastor. 1993. "Patch Formation and Maintenance in an Old Growth Hemlock-Hardwood Forest." *Ecology* 74: 513–527.

Fritts, H. C. 1976. *Tree Rings and Climate*. London, UK: Academic Press.

Galván, J. D., J. J. Camarero, C. Ginzler, and U. Büntgen. 2014. "Spatial Diversity of Recent Trends in Mediterranean Tree Growth." *Environmental Research Letters* 9(8): 084001.

Gill, R. M. A., and V. Beardall. 2001. "The Impact of Deer on Woodlands: The Effects of Browsing and Seed Dispersal on Vegetation Structure and Composition." *Forestry: An International Journal of Forest Research* 74(3): 209–218.

Gómez-García, D., Á. J. de Aguirre Juana, R. Jiménez Sánchez, and C. Manrique Magallón. 2023. "Shrub Encroachment in Mediterranean Mountain Grasslands: Rate and Consequences on Plant Diversity and Forage Availability." *Journal of Vegetation Science* 34(1): e13174.

Grissino-Mayer, H. D. 2001. "Evaluating Crossdating Accuracy: A Manual and Tutorial for the Computer Program COFECHA." *Tree-Ring Research* 57: 205–221.

Guisan, A., S. B. Weiss, and A. D. Weiss. 1999. "GLM Versus CCA Spatial Modeling of Plant Species Distribution." *Plant Ecology* 143(1): 107–122.

Harms, K., R. Condit, S. P. Hubbell, and R. B. Foster. 2001. "Habitat Associations of Trees and Shrubs in a 50-Ha Neotropical Forest Plot." *Journal of Ecology* 89(6): 947–959.

Hesselbarth, M. 2021. "Shar: A R Package to Analyze Species-Habitat Associations Using Point Pattern Analysis." *Journal of Open Source Software* 6(67): 3811.

Hesselbarth, M. H. K., and K. Wiegand. 2024. "A Simulation Study Comparing Common Methods for Analyzing Species–Habitat Associations of Plants." *Journal of Vegetation Science* 35: e13243.

Hijmans, R. 2025. "raster: Geographic Data Analysis and Modeling." R Package Version 3.6–32. https://github.com/rspatial/raster

Hoersch, B., G. Braun, and U. Schmidt. 2002. "Relation between Landform and Vegetation in Alpine Regions of Wallis, Switzerland. A Multiscale Remote Sensing and GIS Approach." *Computers, Environment and Urban Systems* 26(2): 113–139.

Illian, J., A. Penttinen, H. Stoyan, and D. Stoyan. 2008. *Statistical Analysis and Modelling of Spatial Point Patterns* 553. Chichester: John Wiley & Sons.

Kolb, A., and M. Diekmann. 2005. "Effects of Life-History Traits on Responses of Plant Species to Forest Fragmentation." *Conservation Biology* 19(3): 929–938.

Legendre, L., and P. Legendre. 1998. *Numerical Ecology: Developments in Environmental Modelling*. New York: Elsevier.

Legendre, P., and M. J. Fortin. 1989. "Spatial Pattern and Ecological Analysis." *Vegetatio* 80: 107–138.

Lombardo, E., B. Svetlana, D. Gianniantonio, and G. Venturella. 2020. "Distribution, Ecological Role and Symbioses of Selected Shrubby Species in the Mediterranean Basin: A Review." *Plant Biosystems – An International Journal Dealing with all Aspects of Plant Biology* 154(4): 438–454.

Lüdecke, D., M. Ben-Shachar, I. Patil, P. Waggoner, and D. Makowski. 2021. "performance: An R Package for Assessment, Comparison and Testing of Statistical Models." *Journal of Open Source Software* 6(60): 3139.

Maestre, F. T., M. A. Bowker, M. D. Puche, M. B. Hinojosa, I. Martínez, P. García-Palacios, A. P. Castillo, et al. 2009. "Shrub Encroachment Can Reverse Desertification in Semi-Arid Mediterranean Grasslands." *Ecology Letters* 12(9): 930–941.

Martínez-Sastre, R., F. Ravera, J. A. González, C. López Santiago, I. Bidegain, and G. Munda. 2017. "Mediterranean Landscapes under Change: Combining Social Multicriteria Evaluation and the Ecosystem Services Framework for Land Use Planning." *Land Use Policy* 67: 472–486.

McIntyre, S., and R. Hobbs. 1999. "A Framework for Conceptualizing Human Effects on Landscapes and Its Relevance to Management and Research Models." *Conservation Biology* 13(6): 1282–92.

Médail, F., A.-C. Monnet, D. Pavon, T. Nikolic, P. Dimopoulos, G. Bacchetta, J. Arroyo, et al. 2019. "What Is a Tree in the Mediterranean Basin Hotspot? A Critical Analysis." *Forest Ecosystems* 6(1): 17.

Moeur, M. 1991. *Spatial Variation in Conifers Regenerating Beneath Old-Growth Forest Canopies*. Seattle: University of Washington.

Morera, B., P. J. Garrote, T. Wiegand, D. Ayllón, and J. M. Fedriani. 2025. "Invariant Spatial Pattern across Mediterranean Scrublands in the Iberian Pear (*Pyrus bourgaeana*)." *Ecology and Evolution* 15(1): e70757.

Muñoz Garmendia, F., and C. Navarro Aranda. 1998. *Flora Ibérica: Plantas vasculares de la Península Iberica e Islas Baleares, vol. 6. Rosaceae*. Madrid: Real Jardín Botanico-CSIC.

Muñoz, M. C., H. M. Schaefer, K. Böhning-Gaese, and M. Schleuning. 2017. "Positive Relationship between Fruit Removal by Animals and Seedling Recruitment in a Tropical Forest." *Basic and Applied Ecology* 20: 31–39.

Myers, N., R. A. Mittermeier, C. G. Mittermeier, G. A. B. da Fonseca, and J. Kent. 2000. "Biodiversity Hotspots for Conservation Priorities." *Nature* 403(6772): 853–58.

Nadal-Romero, E., K. Petrlic, E. Verachtert, E. Bochet, and J. Poesen. 2014. "Effects of Slope Angle and Aspect on Plant Cover and Species Richness in a Humid Mediterranean Badland." *Earth Surface Processes and Landforms* 39(13): 1705–16.

Olthoff, A. E., C. Gómez, J. G. Alday, and C. Martínez-Ruiz. 2018. "Mapping Forest Vegetation Patterns in an Atlantic–Mediterranean Transitional Area by Integration of Ordination and Geostatistical Techniques." *Journal of Plant Ecology* 11(1): 114–122.

Parry, J., and D. H. Locke. 2024. "sfdep: Spatial Dependence for Simple Features." R Package Version 0.2.4, https://github.com/josiahparry/sfdep, https://sfdep.josiahparry.com.

Peñuelas, J., and J. Sardans. 2021. "Global Change and Forest Disturbances in the Mediterranean Basin: Breakthroughs, Knowledge Gaps, and Recommendations." *Forests* 12(5): 603.

Peñuelas, J., J. Sardans, I. Filella, M. Estiarte, J. Llusià, R. Ogaya, J. Carnicer, et al. 2017. "Impacts of Global Change on Mediterranean Forests and Their Services." *Forests* 8(12): 463.

Peterson, C. J., and S. T. A. Pickett. 2000. "Patch Type Influences on Regeneration in a Western Pennsylvania, USA, Catastrophic Windthrow." *Oikos* 90(3): 489–500.

Pommerening, A., G. Zhang, and X. Zhang. 2021. "Unravelling the Mechanisms of Spatial Correlation between Species and Size Diversity in Forest Ecosystems." *Ecological Indicators* 121: 106995.

Pressey, R. L., M. Cabeza, M. E. Watts, R. M. Cowling, and K. A. Wilson. 2007. "Conservation Planning in a Changing World." *Trends in Ecology & Evolution* 22(11): 583–592.

Quintas-Soriano, C., A. Buerkert, and T. Plieninger. 2022. "Effects of Land Abandonment on Nature Contributions to People and Good Quality of Life Components in the Mediterranean Region: A Review." *Land Use Policy* 116: 106053.

Rasmussen, K. K., and J. Kollmann. 2007. "Genetic Diversity, Spatial Patterns, and Growth of Root Sprouts in a Temperate Tree at the Northern Distribution Limit." *Ecoscience* 14(2): 250–58.

Ripley, B. D. 1981. *Spatial Statistics*. New York: John Wiley & Sons.

Rivest, D., V. Rolo, L. López-Díaz, and G. Moreno. 2011. "Shrub Encroachment in Mediterranean Silvopastoral Systems: Retama Sphaerocarpa and Cistus Ladanifer Induce Contrasting Effects on Pasture and Quercus Ilex Production." *Agriculture, Ecosystems & Environment* 141(3): 447–454.

Robin, V., S. Dreibrodt, and B. Talon. 2021. "The Mediterranean Old-Growth Forests: Anomalies or Relicts? The Contribution of Soil Charcoal Analysis." *Forests* 12(11): 1541.

Rozas, V. 2003. "Regeneration Patterns, Dendroecology, and Forest-Use History in an Old-Growth Beech–Oak Lowland Forest in Northern Spain." *Forest Ecology and Management* 182(1): 175–194.

Rozas, V., R. Zas, and A. Solla. 2009. "Spatial Structure of Deciduous Forest Stands with Contrasting Human Influence in Northwest Spain." *European Journal of Forest Research* 128(3): 273–285.

Sillero, N., S. Arenas-Castro, U. Enriquez-Urzelai, C. Gomes Vale, D. Sousa-Guedes, F. Martínez-Freiría, R. Real, and A. M. Barbosa. 2021. "Want to Model a Species Niche? A Step-by-Step Guideline on Correlative Ecological Niche Modelling." *Ecological Modelling* 456: 109671.

Stein, A., and H. Kreft. 2015. "Terminology and Quantification of Environmental Heterogeneity in Species-Richness Research." *Biological Reviews* 90(3): 815–836.

Stokes, M. A. 1968. In *An Introduction to Tree-Ring Dating [by] Marvin A. Stokes and Terah L. Smiley*, edited by T. L. Smiley. Chicago: Chicago, University of Chicago Press.

Stoyan, H., and D. Stoyan. 1994. "Fractals, Random Shapes and Point Fields." In *Methods of Geometrical Statistics*, Vol. 14, 408. New York: John Wiley & Sons.

Swetnam, T. W., M. A. Thompson, and E. K. Sutherland. 1985. "Using Dendrochronology to Measure Radial Growth of Defoliated Trees." US Department of Agriculture, Forest Service, Cooperative State Research Service.

Upton, G. J., and B. Fingleton. 1985. "Spatial Data Analysis by Example." In *Point Pattern and Quantitative Data*. Chichester: Wiley and Sons.

Valdés, B., S. Talavera, and E. Fernández-Galiano. 1987. "*Pyrus bourgaeana* (Decne)." In *Flora Vascular de Andalucía Occidental (Ed. Ketres). Pyrus bourgaeana (Decne)*, Vol. VI, edited by S. y. F.-G. E. Talavera, 39. Sevilla: Consejería de Medio Ambiente, Junta de Andalucía.

Van Niel, K. P., S. W. Laffan, and B. G. Lees. 2004. "Effect of Error in the DEM on Environmental Variables for Predictive Vegetation Modelling." *Journal of Vegetation Science* 15: 747–756.

Vik, U., M. H. Jørgensen, H. Kauserud, I. Nordal, and A. K. Brysting. 2010. "Microsatellite Markers Show Decreasing Diversity but Unchanged Level of Clonality in Dryas Octopetala (Rosaceae) with Increasing Latitude." *American Journal of Botany* 97(6): 988–997.

Wang, X., T. Wiegand, A. Wolf, R. Howe, S. J. Davies, and Z. Hao. 2011. "Spatial Patterns of Tree Species Richness in Two Temperate Forests." *Journal of Ecology* 99(6): 1382–93.

Weiner, C. N., M. Werner, K. Eduard Linsenmair, and N. Blüthgen. 2011. "Land Use Intensity in Grasslands: Changes in Biodiversity, Species Composition and Specialisation in Flower Visitor Networks." *Basic and Applied Ecology* 12(4): 292–99.

Wiegand, T., and K. A. Moloney. 2013. *Handbook of Spatial Point-Pattern Analysis in Ecology*, 1st ed. New York: Chapman and Hall/CRC.

Wiegand, T., K. A. Moloney, J. Naves, and F. Knauer. 1999. "Finding the Missing Link between Landscape Structure and Population Dynamics: A Spatially Explicit Perspective." *The American Naturalist* 154(6): 605–627.

Zhang, C., X. Zhao, L. Gao, and K. von Gadow. 2010. "Gender-Related Distributions of *Fraxinus mandshurica* in Secondary and Old-Growth Forests." *Acta Oecologica* 36(1): 55–62.

Zuleta, D., S. E. Russo, A. Barona, J. S. Barreto-Silva, D. Cardenas, N. Castaño, S. J. Davies, et al. 2020. "Importance of Topography for Tree Species Habitat Distributions in a Terra Firme Forest in the Colombian Amazon." *Plant and Soil* 450(1): 133–149.

SUPPORTING INFORMATION

Additional supporting information can be found online in the Supporting Information section at the end of this article.

How to cite this article: Arenas-Castro, Salvador, and Diego Jordano-Barbudo. 2026. "Microtopography and Land Management Drive the Spatial and Population Structures of a Mediterranean Keystone Species." *Ecosphere* 17(1): e70506. https://doi.org/10.1002/ecs2.70506